
This is an electronic reprint of the original article.
This reprint may differ from the original in pagination and typographic detail.

Alanne, Kari; Liimatainen, Heikki

Design implications of the electrification of passenger vehicle stock on renewable energy integration in Finnish apartment buildings

Published in:
Sustainable Cities and Society

DOI:
[10.1016/j.scs.2019.101507](https://doi.org/10.1016/j.scs.2019.101507)

Published: 01/05/2019

Document Version
Peer-reviewed accepted author manuscript, also known as Final accepted manuscript or Post-print

Published under the following license:
CC BY-NC-ND

Please cite the original version:
Alanne, K., & Liimatainen, H. (2019). Design implications of the electrification of passenger vehicle stock on renewable energy integration in Finnish apartment buildings. *Sustainable Cities and Society*, 47, Article 101507. <https://doi.org/10.1016/j.scs.2019.101507>

This material is protected by copyright and other intellectual property rights, and duplication or sale of all or part of any of the repository collections is not permitted, except that material may be duplicated by you for your research use or educational purposes in electronic or print form. You must obtain permission for any other use. Electronic or print copies may not be offered, whether for sale or otherwise to anyone who is not an authorised user.

Design implications of the electrification of passenger vehicle stock on renewable energy integration in Finnish apartment buildings

Kari Alanne^{*1}, Heikki Liimatainen²

¹*Department of Mechanical Engineering, School of Engineering, Aalto University, PO Box 14400, FI-00076 Aalto, Finland*

²*Transport Research Centre Verne, Tampere University, PO Box 600, 33014 Tampere University, Finland*

Abstract

The dense network of charging stations is imperative for promoting the electrification of vehicles. Generating and distributing transportation energy via buildings' energy systems can be considered a necessity for the transition to electric vehicles (EV). In this paper, it is argued that transportation energy should be included in buildings' energy balance when designing building-integrated renewable energy system with zero-energy goals. Hence, a statistically inspired, occupant-specific model is developed to quantify the transportation energy demand on the basis of personal mobility requirements and to convert it into the EVs' charging demand. The usability of the model is shown through a case study, where a new Finnish apartment building with building-integrated solar photovoltaic (PV) system is investigated. The occupants' personal mobility requirements are predicted and analyzed in the present conditions and three future scenarios describing the electrification of the Finnish passenger vehicle stock. The results support the hypothesis. Even the moderate electrification of the Finnish vehicle stock (250,000 EVs) results in the share of transportation energy of 6-10% in the building's net energy demand. Correspondingly, to maintain the building's energy performance comparable to the case with no vehicle charging included, the size of the building-integrated PV system should be increased by 34%.

Keywords: zero-energy buildings, transportation, renewable energy

1 Introduction

Buildings in Europe account for 41% of the final energy consumption, followed by transport (32%), and industry (25%) [1]. In the EU Directive 2010/31/EU, the EU Member States have agreed that by the end of 2020 all new buildings are to be nearly zero-energy buildings [2]. The Paris Agreement requires pushing energy performance levels significantly beyond the requirements recorded in the current EU building codes, and also realizing Positive Energy Districts by 2050. Consequently, the related research and development has extended its scope from single buildings towards communities [3, 4]. The potentialities of an integrated approach linking transportation and building energy consumptions have been shown [5]. The literature acknowledges the role of vehicles as equipment to store and exchange energy with buildings or energy grids [6]. The evolution of the future transportation signifies connectivity, automation, and sharing [7]. In tandem with shared ownership, the dividing line between housing and mobility will dim [8].

Given that the lack of a dense network of charging stations is one of the key hindrances for the electrification of vehicles, the improvement of home-charging abilities is urgency rather than an option. Again, the installation of home charging stations affects the buildings' energy balance and thus the sizing and operation of building-integrated renewable energy systems. The designers and policy-makers will have to determine whether to require more building-integrated renewable energy to cover as much of the transportation energy demand by on-site resources as possible or to alleviate the requirements of nearly zero-energy levels understanding that a fraction of the buildings' energy demand is factually represented by transportation.

Several recent researches investigate calculating and combining transportation energy in life-cycle, emission and cost evaluations at the community level [9-14]. Formulating transportation energy demand profiles utilize numerous approaches, such as empirical surveys and Geographic Information Systems (GIS) [15], activity-based modeling [16] and artificially generated databases,

where the user behavior is randomized [9]. Instead, there is a lack of standardized, transparent and simple enough methods to integrate the vehicle-specific energy demands and occupant-specific mobility requirements in single buildings' energy balance to address their implications for the early-stage design of buildings' energy systems. Correspondingly, the design implications of variations in occupants' mobility requirements, the degree of electrification of the vehicle stock, the degree of utilization of home charging, as well as vehicle automation and ridesharing are not yet well-known.

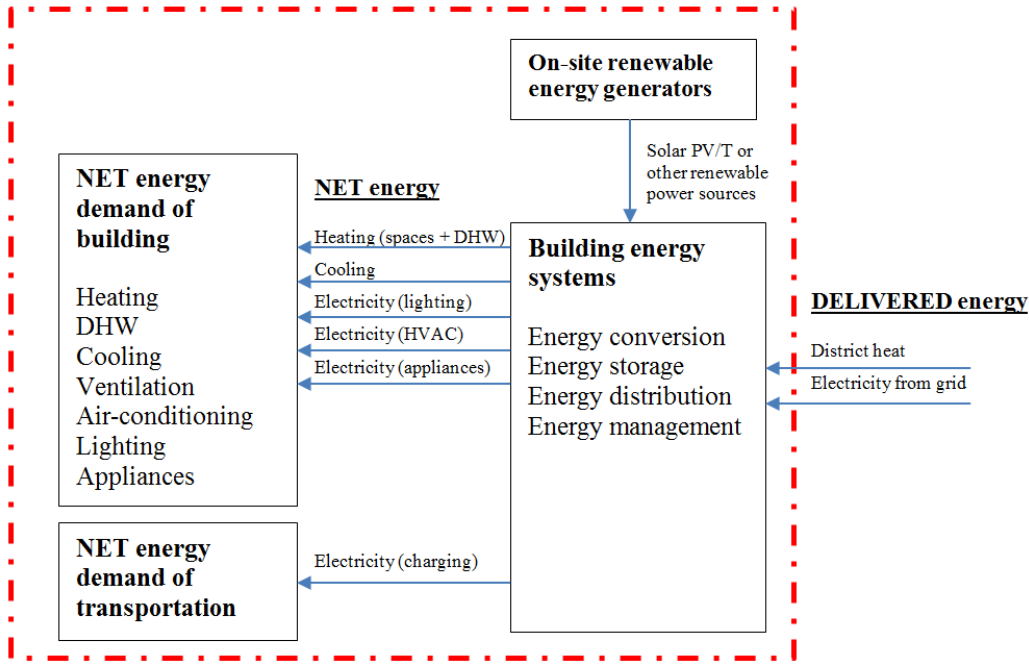
To fill some of the aforementioned research gaps, a statistically inspired, occupant-specific model is developed in the present study to quantify the transportation energy demand in a building's energy balance as EVs' charging requirement. The suggested approach only relies on the number of occupants and routinely collected statistical data on national transportation, wherefore it is useful in the early-stage design, compared, for example, to an activity-based approach, which requires more detailed occupant profiling [16]. Applying building-integrated power storage and unidirectional power transfer (B2V), the proposed approach circumvents the need to evaluate the mobility requirement on hourly basis. The electrical demands of lighting and appliances are modeled following the specific demand acquired from the building code. The heating and cooling demands are calculated on hourly basis using a dynamic whole-building simulation tool. The model is implemented in a case study, where the personal mobility requirements associated with a new Finnish apartment building are quantified and analyzed in both the present conditions and in three future scenarios that depict the degree of electrification of the Finnish passenger vehicle stock with moderate, ambitious and hypothetical expectations. Hence, the study represents an effort to outline the worst case scenarios for designers to be prepared for in the Finnish context and to evaluate their potential impacts on the buildings' energy performance.

2 Methodology

2.1 System boundary and the key energy performance indicators

Approaching zero-energy goals calls for the best practices regarding energy efficiency and renewable energy integration [2]. Design solutions aim at the least possible (non-renewable primary) energy consumption and life-cycle costs [17]. The suggested methodology aims at assessing the impact of electric transportation on the required capacity of on-site renewable energy generators and the on-site energy storage capacity. The size (and occupancy) of a building is chosen large enough in order to level the individual preferences of occupants. In that sense, the building can be also considered a (small) community or neighborhood.

The model is based on the technical definition of nearly zero energy buildings by the Federation of European Heating, Ventilation and Air Conditioning Associations (REHVA) [18]. However, the transportation energy demand is included in a building's energy balance as shown in Fig. 1. Only district heat and electricity are delivered from the grid. Cooling is realized by either electrically-driven or free cooling systems. No energy surplus is allowed, but all the on-site renewable energy is stored and used within the system boundary. The approach is justified by the intention is to avoid burdening power grids. Again, it is presumed that there is no bi-directional power exchange between vehicles and building energy systems.



System boundary of delivered energy on-site

Figure 1. System boundary of a building with net energy demand of transportation included.

The building energy performance is indicated by two key indicators. Firstly, the non-renewable primary energy consumption is quantified by the energy performance indicator (EP , in Finland known as the ‘ E -value’), which is defined as the annual delivered energy demand as calculated per heated net interior area of the building. Referring to Fig. 1, it is calculated from

$$EP = \frac{\sum_i w_i E_i}{A_{net}} \quad (1),$$

where w_i is the specific weight coefficient to convert the annual demand for the i -th delivered energy form (E_i) into primary energy at the source and A_{net} is the net heated area of the building.

The specific values of the weight coefficients depend on the properties of the local energy supply chain (energy mix, efficiency) and they are defined and agreed in terms of national policy making.

Since the maximal use of local renewable energy resources is pursued with a simultaneous intention to restrain grid interaction, it is justifiable to determine the on-site energy fraction (OEF) along with

the EP (*E*-value) [19]. The OEF is defined as the proportion of the on-site demand covered by the on-site energy generation as shown in Fig. 2 and it is calculated from

$$OEF = \frac{\int_{t_1}^{t_2} \text{MIN}[G(t); L(t)]dt}{\int_{t_1}^{t_2} L(t)dt}; \quad 0 \leq OEF \leq 1 \quad (2)$$

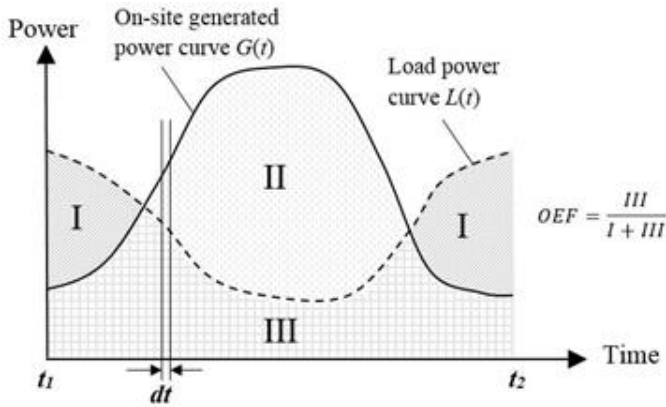


Figure 2. General principle of calculating the OEF.

2.2 Calculation of transportation energy demand

2.2.1 Net energy demand

In the proposed model, the net energy demand of transportation is calculated on the basis of occupant-specific transportation energy demand, defined as the amount of energy required to transport one passenger over one kilometer and unitized as kilowatt hours per passenger kilometer (p-km).

The occupant-specific transportation energy demand depends on the type of transportation equipment and its prime mover, whereas the governing variables are occupancy (load) and the mode of transportation. For passenger cars, equipment-specific energy demands are routinely determined for both empty and full vehicles. They are also determined for both highway driving and urban driving, because these are remarkably different modes of transportation. The aforementioned data are collected into databases using representative manufacturer data and, when applicable, the

statistics of the regional vehicle stock compositions. In the present study, the equipment-specific energy demands are acquired from the LIPASTO calculation system, which has been created and collected by the VTT Research Centre of Finland following the principles described in the European standard “*Methodology for calculation and declaration of energy consumption and GHG emissions of transport services (freight and passengers)*” (EN 16258) [20]. Table 1 exemplifies the specific energy demand data for passenger cars according to the LIPASTO database.

Table 1. Specific energy demands of passenger cars with various prime movers [20].

Prime mover	Highway driving Occupancy 1.9 persons		Urban driving Occupancy 1.3 persons	
	Equipment-specific [kWh/km]	Occupant-specific [kWh/p-km]	Equipment-specific [kWh/km]	Occupant-specific [kWh/p-km]
Diesel	0.51	0.27	0.81	0.35
Gasoline	0.56	0.30	0.83	0.64
Electricity	0.20	0.11	0.17	0.13
High-blend ethanol	0.52	0.28	0.75	0.57
Gas	0.49	0.26	0.68	0.53

The data in Table 1 also illustrates the relationship between equipment-specific and occupant-specific transportation energy demand. In highway driving (occupancy 1.9 persons per vehicle), for example, the occupant-specific energy demand of electric cars is $0.20 / 1.9 = 0.11$ kWh/p-km. Again, the occupant-specific energy demand is calculated for varying modes of transportation as weighted average, where pre-defined weight coefficients represent the fractions of highway driving and urban driving. For example, assuming that 27% of the driving distance is urban driving, the occupant-specific transportation energy demand for electric cars is $0.27 \cdot 0.13 + (1 - 0.27) \cdot 0.11 \approx 0.11$ kWh/p-km.

The transportation energy demand calculation also requires mapping the occupant-specific personal mobility requirements (travel distances) on daily basis by surveying a statistically significant sample of respondents populating the given type of building (cluster, district) located on a specific type of region or neighborhood. The calculation can be generalized to various building types

presuming that the population is large enough and representative. If the number of occupants is small, a more descriptive mobility profile would require a case-specific travel survey.

The present study makes use of the results of the latest National Travel Survey (NTS), which is conducted on a regular basis by the Finnish Transport Agency [21]. The intention is to provide an overview of the mobility and affecting factors, as well as demographic, regional and temporal variations of passenger trips. Table 2 summarizes the daily travel distances as a result of the NTS 2016 for various types of neighborhoods and transportation equipment. The numbers in Table 2 have been adapted to standardized population to eliminate the demographic differences between various neighborhoods.

Table 2. Daily travel distances for standardized population according to NTS 2016 [21].

Equipment	Helsinki metropolitan area [p-km/day]	Other big cities [p-km/day]	Medium-size cities [p-km/day]	Small cities [p-km/day]	Other municipalities [p-km/day]
Passenger car	21.8	27.1	32.8	36.1	45.1
Rail	3.3	2.8	2.9	0.7	0.9
Bus	3.0	2.8	2.4	2.3	1.7
Bicycle	0.7	1.1	0.7	0.6	0.5
Pedestrian	1.1	1.2	0.9	0.9	0.7

Given that the number of occupants is known, the total daily travel distance is obtained by multiplying the daily travel distance of one occupant by the total number of occupants. Again, the total travel distance can be allocated to various equipment (e.g. passenger car, public transportation etc.) presuming that the travel demand by equipment is known, as in Table 2.

2.2.2 Delivered energy demand

The net energy demand of transportation (as defined Section 2.2.1) includes the fraction of transportation energy demand that is distributed via the buildings' own energy systems. It also represents the energy input to the transportation equipment, including the energy conversion and storage losses onboard (well-to-wheel efficiency). Hence, the delivered transportation energy

demand is the sum of the net transportation energy and the energy losses of the power storage, conversion and transmission inside the system boundary (Fig. 1), which originate from charging EVs on-site.

Given that assessing the design implications addresses the hardest expected conditions (the largest incremental energy demand in comparison with the case where no transportation energy is included in the system's energy balance), it should be assumed that charging of EVs at external charging stations is not accounted, but the transportation energy demand as whole is distributed via buildings' energy systems and home charging stations.

In the suggested model, the daily net energy demand of transportation is converted into hourly delivered energy demand by presuming that the charging period starts at the moment of time t_{1c} and ends at t_{2c} . The hourly delivered energy demand ($E_{del,t}$), which also equals to the hourly mean power demand of the charging system, is calculated from

$$E_{del,t} = \frac{E_{net,t}}{\eta_c (t_{2c} - t_{1c})} \quad (3)$$

where $E_{net,t}$ is the daily net energy demand of transportation, η_c is the efficiency of the charging system and t_{1c} and t_{2c} are the hours of time when the charging starts and stops, respectively.

2.3 Calculation of building energy demand

2.3.1 Net energy demand

The hourly net heating demand of spaces and ventilation as well as the cooling demand is calculated using a dynamic building energy simulation tool. The dynamic IDA-ICE building energy simulation software (version 4.7) is preferred, since it allows modeling multi-zone buildings, HVAC systems, internal loads, outdoor climate, among others, and provides dynamic simulation of heat and airflows with a variable time-step. Heat balance equations are solved by the finite difference method. The building construction model with various geometries can be drawn or imported from CAD

programs via IFC files, whereas hourly climate files are used to acquire the input variables related to weather, such as external temperatures, relative humidity, and solar irradiation. Here, the climatic data are based on the updated test reference year 2012 (TRY2012) weather data of the Finnish climatic zone I (Southern Finland).

The internal heat gains from occupants, household equipment and lighting are acquired using the standardized specific internal gains if no more specific data are available. In the present study, they are determined using the National Building Code of Finland (NBCF) part D3 (2012) and applied to all rooms throughout a target building [22]. The heat gains due to the charging system for electric vehicles are assumed to be included in the standardized specific internal gains. Further details on the implementation of the above approach in the present study are provided in Section 3.1.

2.3.2 Delivered energy demand

The delivered energy demands are found out by post-processing the numerical results from the procedures explained in Sections 2.2.1 – 2.3.1. The calculation procedure entails two steps and it is implemented on hourly basis using a spreadsheet application.

The first step is to determine the on-site energy generation from renewable energy sources. Here, the useful solar thermal energy is obtained directly from the whole-building simulation, including the simulated hourly incident radiations and system temperatures. The building-integrated PV power generation is modeled by multiplying the simulated hourly incident radiation per square meter by the active PV area and by an actual system efficiency, which takes into account the impact of operational conditions and system losses. The system efficiency is chosen to represent the experienced performance of the commercial state-of-the-art technology.

The second step is to solve the hourly delivered energy required to balance the demand and supply. To that end, the difference between of the on-site generation and the demand of the i -th energy type is solved from

$$\Delta E_i = E_{gen,i} - E_{d,i} \quad (4)$$

where $E_{gen,i}$ is the energy generation from on-site renewable energy sources and $E_{d,i}$ is the sum of energy demands of a certain energy type for the i -th hour. The sum ($E_{d,i}$) includes all the building-related energy demands and the delivered transportation energy demand as defined in Section 2.2.2 ($E_{del,t}$). As Eq. (4) implies, energy surplus is realized when $\Delta E_i > 0$. Correspondingly, energy shortage occurs, when $\Delta E_i < 0$. The absolute state-of-charge of the energy storage for the i -th hour is calculated from

$$ASOC_i = ASOC_{i-1} + \Delta E_i \quad (5)$$

In Eq. (5), the value of ΔE_i for the current hour (i) is used and discharging below zero ($ASOC_{n,i} < 0$) is prevented by if-then-else rules. Discharging the storage ($\Delta E_i < 0$) is penalized by multiplying it by the round-trip efficiency of the energy storage, whereas the storage losses are compensated by importing a corresponding amount of energy from outside of the system boundary (grids). Again, the highest value of $ASOC_i$ within a whole-year simulation represents the required capacity of the on-site energy storage and thus it is used as a reference value for system sizing. Even though the largest ΔE_i stands for the maximal mean discharging power, it provides quite a poor sizing reference, however, because it does not take into account possible instant peak powers. Hence, the case study does not apply to the power-based sizing.

The heat conversion and distribution losses inside the system boundary are accounted by dividing the simulated net thermal energy demand by the annual efficiencies of the corresponding systems, which are retrieved from the National Building Code of Finland (NBCF) part D5 (2012) [23]. In the case where the primary heat source is a heat pump, the heat demand is converted into the electrical

power demand through division by the seasonal performance factor (SPF). Correspondingly, the electrical power demand of cooling is calculated by dividing the simulated net cooling demand by the seasonal coefficient of performance (SCOP) of the cooling system, which is provided by the NBCF/D5 (2012), as well.

3 Case study

3.1 Target building

The case study utilizes an apartment building located in Helsinki metropolitan area. The building consists of five storeys and a cellar including a heated parking garage. The computational net heated area is 3570.9 m². The building geometry is illustrated in Fig. 3, whereas the key specifications of the structures are in Table 3. The data in Table 3 refers to a real building to be constructed in Järvenpää (a town located in Helsinki metropolitan area). The target building is specified with details in the final report of the development project “*HP4NZEZB – Heat Pump Concepts for Nearly Zero Energy Buildings*” [24].



Figure 3. The geometry of the target building.

Table 3. Structural specifications of the target building.

Structure	Specification
External wall	U-value: $U = 0.13 \text{ Wm}^{-2}\text{K}^{-1}$
Roof	U-value: $U = 0.09 \text{ Wm}^{-2}\text{K}^{-1}$
Base floor	U-value: $U = 0.27 \text{ Wm}^{-2}\text{K}^{-1}$ Connected to ground
Internal walls between staircases and apartments	U-value: $U = 0.60 \text{ Wm}^{-2}\text{K}^{-1}$
Internal walls between apartments	U-value: $U = 2.09 \text{ Wm}^{-2}\text{K}^{-1}$
Intermediate floor	U-value: $U = 1.73 \text{ Wm}^{-2}\text{K}^{-1}$
External door	U-value: $U = 1.00 \text{ Wm}^{-2}\text{K}^{-1}$
Windows	U-value: $U = 0.80 \text{ Wm}^{-2}\text{K}^{-1}$ g-value: $g = 0.37$ ST-value: $ST = 0.31$
Integrated window shading	Blinds between the outer panes
Air-tightness	$n_{50} = 0.40 \text{ h}^{-1}$ $q_{50} = 1.43 \text{ m}^3\text{h}^{-1}\text{m}^{-2}$

The target building has 124 occupants, which is the maximum allowable occupancy for this building type according to the NBCF/D3 (2012) [22]. This high occupancy has been chosen to address the extreme conditions for sizing the building's energy systems. On the other hand, the reliability of the statistical approach improves with the increase of the representative sample size.

The specific energy demand including the internal heat gains for lighting, persons and household equipment, are acquired from the NBCF/D3 (2012) [22]. The specific heat gain for occupants is 3.0 Wm^{-2} , whereas the specific powers of lighting and appliances are 11.0 Wm^{-2} and 4.0 Wm^{-2} , respectively. The aforementioned values are reduced to depict the actual demand by multiplying them by the utilization rates. The utilization rate for occupants and appliances is 0.6 and for lighting it is 0.1, whereas the reduced heat gain is constant throughout the year. Thus, the mean hourly power is 8570 W for appliances and 3928 W for lighting and it is applied for each day of the year, because no data with higher resolution are available.

The demand profile of the domestic hot water (DHW) is based on measured consumption in a Finnish apartment building ($0.5 \text{ m}^3\text{m}^{-2}\text{y}^{-1}$). There is a DHW circulation system in the building (flow rate 0.13 Ls^{-1}) and the supply/return temperatures are 58/55 °C. The piping is assumed well-insulated. The distribution of hourly mean values of DHW heating demand over one day is shown

in Fig.4. It is also worth mentioning that in the present study, the DHW heating demand is high in comparison with space heating demand, since the building envelope and its systems have chosen with an aim at high energy efficiency, whereas the consumption habits of the occupants are not affected and no particular energy efficiency improvements have been implemented.

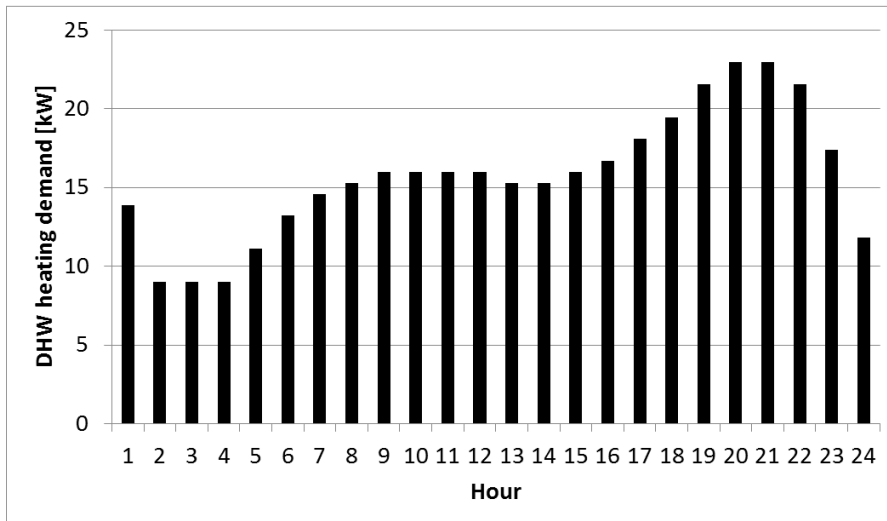


Figure 4. DHW heating demand profile for one day.

3.2 Optional energy systems for the target building

The heat distribution system is water-based (hydronic). It is a low-temperature radiator and floor heating system, the dimensioning temperatures for supply and return being 45°C and 35°C, respectively. The set-points for heating are 17.0°C (ON) and 21.0°C (OFF). The set-point temperature for the supply water is adjusted according to the external temperature. The cooling system is water-based (supply/return temperatures 10/15°C), as well, and there is a cooling coil in the supply air duct. The building is equipped with a mechanical supply and exhaust ventilation system, which operates continuously. The supply and exhaust air flow rate is 0.5 Ls⁻¹m⁻² and the system contains a heat recovery equipment (temperature efficiencies 80% and 75% for residential zones and the parking garage, respectively). The supply air temperature 18.0°C is maintained throughout the year, whereas the cooling period starts on June 1 and ends on August 31. Cooling starts when the room temperature exceeds 27.0°C.

Two optional heating systems are considered. The first option is district heating, the annual heat distribution efficiency of which is 90% for spaces and 97% for DHW according to the NBCF/D5 (2012) [23]. The cooling system is a mechanical water chiller system with the SCOP = 3.0. The second option is a ground source heat pump (GSHP) system with the SCOP = 2.3. Here, the source of cooling energy is free cooling with boreholes (simulated SCOP = 30, containing the electrical demand of circulation pumps).

When dimensioning the integrated renewable energy systems, the sum of the installed PV and ST areas may not exceed 50% of the building's total roof area (696 m²), since otherwise the panels and collectors would begin to shade each other. Therefore, the reference design (transportation energy neglected) includes the target building equipped with 200 m² of solar PV panel with the system efficiency of 19%. Moreover, there is an option for 78 m² of solar thermal collectors.

The simulation model includes a thermal storage tank, the volume of which is 5000 L, corresponding to the maximum storage capacity of around 290 kWh at the temperature difference of 50°C. The battery energy storage system (BES) includes the lithium-ion-based Tesla Powerpack 1 and/or 2 system, the capacities of which are 100 kWh and 210 kWh, respectively. The round-trip efficiency is assumed to be 88% (manufacturer's note), whereas the maximum discharge rate (power output) is 50 kW.

3.3 Scenarios of electric transportation

The case study describes the evolution of vehicle stock by way of a reference scenario and three future scenarios. The reference scenario (REF) represents the current situation, where transportation energy is either not included in the building's energy balance at all or the fraction of electric vehicles in the vehicle stock is small. The future scenario (1) analyzes the case study with moderate growth in the amount of electric vehicles, whereas the future scenario (2) represents ambitious electrification of passenger transport. The future scenario (3) is hypothetical, including an

assumption of fully electrified vehicle fleet, where the number of vehicles is reduced due to automation and ridesharing. The impact of electric (or electrically assisted) bicycles on the building's annual energy balance and system sizing is evaluated separately.

In the reference scenario, the occupant-specific daily travel distances are taken from the NTS 2016 for the standardized population of Helsinki metropolitan area as shown in Table 2 [21]. For the future scenarios (1-3), the occupant-specific travel distance is predicted on the basis of the data provided by the report of the Prime Minister's Office on the energy efficiency measures to obtain the European climatic and energy targets in 2030 [25]. Making use of the annual percentage change in travel distances, the number of passenger kilometers is predicted to develop by 2030 as follows:

Passenger cars:	21.8 → 22.9 p-km/day (+0.4%/y)
Public transportation (bus + rail):	6.3 → 8.2 p-km/day (+1.9%/y)
Bicycle:	0.7 → 0.9 p-km/day (+1.5%/y)

The percentage of urban driving (street driving) is 27% and that of the highway driving is 73% for each of the analyzed scenarios. The vehicle-specific occupancies in the regular use are as in Table 1 (1.9 for highway driving and 1.3 for urban driving), whereas the numbers are doubled in the ridesharing mode.

Because the scenario analysis requires the occupant-specific electrical energy demands per passenger kilometers, the transportation energy demand is allocated by prime mover. To that end, the total annual driving distance for each prime mover and each vehicle type is mapped. The reference scenario makes use of the statistics for the year 2016, when the total driving distance for gasoline-powered cars was 23,097 million kilometers, whereas for diesel-powered cars it was 16,043 million kilometers [26]. These represent 59% and 41% of the total driving distance, respectively. The contribution of electric passenger cars in the driving distance (31 million kilometers, 0.1%) at the present is close to negligible. For the future scenarios, a forecast is made for the development of the electrically-powered driving distance by 2030. The forecast applies

vehicle-specific annual travel distances by prime mover and by the year of introduction (passenger cars introduced in 1998-2016) in Finland as shown in Fig. 5 [26].

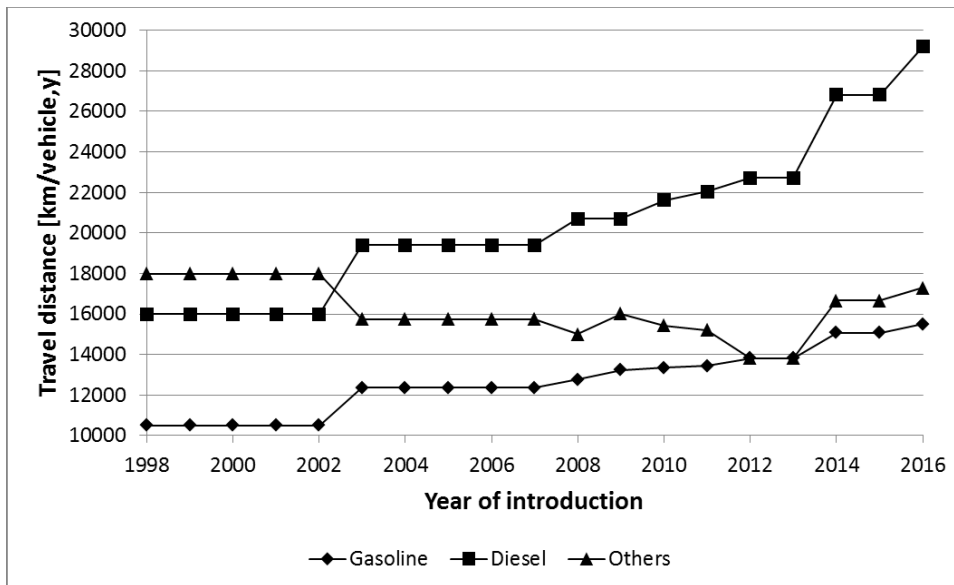


Figure 5. Vehicle-specific travel distances by prime mover and year of introduction [26].

Regarding the predictions relying on the data in Fig. 5, it is assumed that the driving distance related to other prime movers (including electricity) grows as a trend from the year 2010 onwards. The assumption contains moderate expectations regarding the development of technology such as vehicle-integrated battery energy storages as well as the transfer of travel kilometers from gasoline and diesel-powered vehicles to those using alternative prime movers. Hence, the predicted annual travel distance for the electric vehicles introduced in 2030 is 22,450 km per year.

The total driving distances are predicted by multiplying the annual vehicle-specific distances by the number of vehicles in the vehicle stock. The future scenario (1) has been chosen to represent the expectations of the national Energy and Climate Strategy (2016), where it is presumed that there are 250,000 full and plug-in hybrid EVs in the Finnish vehicle stock in 2030. (Here, it is assumed, however, that all the 250,000 vehicles are full EVs.) The future scenario (2) reflects on the expectations pronounced in the recent report “Cost-Efficient Emission Reduction Pathway to 2030” by Sitra, presuming that there are 800,000 electric vehicles in the vehicle stock [27]. The

hypothetical future scenario (3) presumes that the vehicle stock in its entirety is electrically-powered. Here, the total number of vehicles is 1,000,000, whereas the total driving distance is equal to the sum of total driving distances over all the prime movers predicted by Sitra in their report [27]. The assumptions regarding the future scenario (3) are based on the “*Metropolitan Vision of Automatic Transportation*”, where it was estimated that the vehicle-specific travel distance increases from 17,000 to 60,000 km per year due to automation and that the vehicle stock of 1,000,000 cars in total (1/3 of the current vehicle stock) together with public transportation would be sufficient to meet the demand of passenger transportation even when the vehicles are not fully occupied [28]. The key characteristics of the Finnish electric vehicle stock for the scenario analysis are summarized in Table 4.

Table 4. Key characteristics of the Finnish electric vehicle stock for the scenario analysis.

Scenario	Number of EVs in the national vehicle stock	Total annual equipment-specific driving distance [Million km/y]	Percentage of electrically powered transportation in occupant-specific travel distance by passenger cars [%]
REF	844	31	0.1%
1	250,000	5,612	9.8 %
2	800,000	17,958	33.4 %
3	1000,000	53,726	100.0 %

3.4 Results and discussion

3.4.1 Energy performance implications

The annual energy profiles for the target building with calculated on-site energy fractions and the E-values for three (3) alternative energy system configurations (A...C) are summarized in Table 5.

The system configurations are:

- A. District heating, solar PV 200 m², power storage 123 kWh
- B. District heating, solar PV 200 m², solar thermal collectors 78 m², power storage 123 kWh, thermal storage 273 kWh
- C. Ground-source heat pump, solar PV 200 m², power storage 74 kWh

All the energy profiles have been calculated per heated net area of the target building (3570.9 m²). The energy storage demands listed above indicate the highest required storage capacity during the simulation year with the conditions that the excess energy does not have to be exported. The contribution of transportation energy demand is not included in the numbers in Table 5, wherefore the data summarize the energy demand in the reference scenario (REF).

Table 5. Energy profiles of the target building for three energy system configurations.

Configuration	PV-generation [kWh/m ² ,y]	PV on-site [kWh/m ² ,y]	ST on-site [kWh/m ² ,y]	Delivered electricity [kWh/m ² ,y]	Delivered district heat [kWh/m ² ,y]	OEF (e) [-]	E-value [kWh/m ² ,y]
A	11.7	11.5	-	31.8	49.6	0.265	63.0
B	11.7	11.5	15.5	31.8	33.6	0.265	55.0
C	11.7	11.6	-	52.1	-	0.182	62.5

The data in Table 5 indicate that the utilized PV (11.5 kWh/m²,y) remains slightly less than the generated PV (11.7 kWh/m²,y), which is explained by the storage losses. Again, the amount of delivered electricity is remarkably larger for the GSHP heating (52.1 kWh/m²,y) than for district heating (31.8 kWh/m²,y), wherefore also the on-site energy fraction for electricity (OEF(e)) remains lower than in the case of district heating. The impact of solar thermal collectors is revealed by the lower E-value of the Configuration B in comparison with the rest of system configurations. The computational study also implies that the maximum hourly mean discharge power of the building-integrated electrical power storage is 23 kW for the district-heated building and 26 kW for the building heated with an electrically-driven ground-source heat pump (GSHP).

The calculated E-values for the target building are well below the proposed national goals for the nearly zero-energy apartment buildings (116 kWh/m²,y) [29]. It is worth mentioning, however, that here we use the specific weight coefficients updated at the beginning of 2018 (1.2 for electricity and 0.5 for district heating), which are clearly lower than the ones applied to determining the national nearly zero-energy goals (1.7 for electricity and 0.7 for district heating). The weight coefficients do

not affect the application of the suggested methodology as such, even though they have influence on the interpretation of the results.

Given that the percentage of electrically powered transportation in the occupant-specific travel distance by passenger cars in the reference scenario is 0.1% (Table 4), the contribution of EV charging in the building's energy balance is around 100 kWh per year (0.03 kWh/m²,y) and the mean charging power is 40 W. Hence, the amount of delivered electricity increases from 31.8 to 31.9 kWh/m²,y for Configurations A and B. Thus, it can be concluded that the aforementioned increase in the energy flow through the building's energy system does not significantly affect the OEF (e), the E-value or sizing the renewable energy system.

Instead, the elevated home charging demand calculated on the basis of the increase in electrically powered travel distance in the future scenarios (1-3) has a perceptible impact on delivered energy, OEF (e) and the E-value of the building. This is shown in Table 6, where the annual electricity demands of home charging and the amount of delivered electricity with calculated on-site energy fractions and the E-values for the three (3) analyzed system configurations (A...C) in the future scenarios (1-2) are summarized. The results entail an assumption that the charging period lasts seven (7) hours, starting at midnight and ending at 7:00 A.M. In the hypothetical future scenario (3), the operation of the vehicle fleet can be optimized with an aim to maximize the usage of the vehicles and to minimize the costs. Therefore, the results have been calculated applying an evenly distributed charging throughout the hours of a day, wherefore the mean charging power remains low in comparison with the rest of scenarios.

Table 6. Electrical demand, OEF (e) and E-value in the future scenarios (1-3).

Future Scenario 1					
Configuration	Annual EV charging demand [kWh/m ² ,y]	Hourly average EV charging power [kW]	Delivered electricity [kWh/m ² ,y]	OEF (e) [-]	E-value [kWh/m ² ,y]
A	3.6	5.1	35.4	0.244	67.3
B	3.6	5.1	35.5	0.245	59.1
C	3.6	5.1	55.7	0.172	66.8
Future Scenario 2					
Configuration	Annual EV charging demand [kWh/m ² ,y]	Hourly average EV charging power [kW]	Delivered electricity [kWh/m ² ,y]	OEF (e) [-]	E-value [kWh/m ² ,y]
A	12.4	17.3	44.2	0.206	77.9
B	12.4	17.3	43.6	0.208	69.1
C	12.4	17.3	64.5	0.152	77.4
Future Scenario 3					
Configuration	Annual EV charging demand [kWh/m ² ,y]	Hourly average EV charging power [kW]	Delivered electricity [kWh/m ² ,y]	OEF (e) [-]	E-value [kWh/m ² ,y]
A	18.5	7.6	50.2	0.188	85.0
B	18.5	7.6	50.2	0.188	77.0
C	18.5	7.6	70.5	0.142	84.6

The data in Table 6 also reveal that the annual electricity demand of home charging directly raises the delivered electricity demand unless the system sizing is not changed. Depending on system configuration, the charging energy demand represents up to 6-10% of the delivered energy in the future scenario (1). The corresponding percentages for the future scenarios (2) and (3) are 19-28% and 26-37%, respectively. Again, the contribution of charging energy in the building's E-value varies between 6-7% in the future scenario (1), 19-20% in the future scenario (2) and 26-29% in the future scenario (3).

The impact of electric bicycles was assessed with an assumption that the occupant-specific travel distance is 0.9 p-km/day, which represents the predicted travel distance of bicycles in 2030. On the basis of the definitions of the Finnish Transport Safety Agency, these vehicles are allowed to operate at the power of 250 W at maximum, whereas their speed is limited to 25 km/h. In the above conditions, the occupant-specific electrical energy demand would be around 0.01 kWh/p-km on the average, which would result in the annual charging energy demand per heated square meter of 0.2 kWh/m²,y, being minor in comparison with that of passenger cars. Using a more conservative assumption based on Bishop et al. [30], who estimate the normalized mains-to-wheel energy use to

be 0.10 kWh/km for electrical scooters, the corresponding annual charging energy demand with the occupancy of one person per vehicle would grow to 1.3 kWh/m²,y. Again, the E-value would only rise from 63.0 to 64.3 kWh/m²,y and the OEF (e) would be cut from 0.265 to 0.261.

3.4.2 System design implications

On the basis of the results described in Section 3.4.1, it may be concluded that the impacts of the introduction of electrically-driven mobility on the building's E-value and the OEF (e) may appear significant especially if the conditions for achieving the nearly zero-energy goals will be tightened or if the cost-optimal building design (envelope, systems) results in an E-value close to a pre-defined limit value (e.g. 116 kWh/m²,y). Thus, it was estimated how much larger the installed PV area and the power storage capacity should be in comparison with the reference scenario (no transportation included in the building's energy balance) to keep the E-value unchanged. The results are shown in Table 7.

Table 7. Design implications for future scenarios (1-3).

Future Scenario 1						
Configuration	Target E-value [kWh/m ² ,y]	Installed PV [m ²]	Difference to REF [m ²]	Installed power storage [kWh]	Difference to REF [kWh]	OEF (e) [-]
A	63.0	267	+67	212	+89	0.321
B	55.0	263	+63	207	+84	0.319
C	62.5	265	+65	146	+72	0.226
Future Scenario 2						
Configuration	Target E-value [kWh/m ² ,y]	Installed PV [m ²]	Difference to REF [m ²]	Installed power storage [kWh]	Difference to REF [kWh]	OEF (e) [-]
A	63.0	432	+232	774	+651	0.428
B	55.0	432	+232	773	+650	0.428
C	62.5	429	+229	381	+309	0.315
Future Scenario 3						
Configuration	Target E-value [kWh/m ² ,y]	Installed PV [m ²]	Difference to REF [m ²]	Installed power storage [kWh]	Difference to REF [kWh]	OEF (e) [-]
A	63.0	549	+362	1000	+877	0.485
B	55.0	549	+362	1000	+877	0.485
C	62.5	538	+338	664	+592	0.366

The data in Table 7 suggest, for example, that when the target E-value for the future scenario (1), Configuration A is set as the same as the E-value in the reference scenario (REF, 63 kWh/m²,y), the

incremental PV installation of 67 m² (+33.5% larger sizing in comparison with the reference) is required. Correspondingly, the electrical storage capacity must be increased by 89 kWh (+72%) to avoid the export of power into the grid. Due to the above changes in system sizing, the OEF (e) increases from 0.265 to 0.321.

In the future scenario (1), the suggested design implications are technically viable for the analyzed building, taking into account issues such as the free roof area and the availability of various sizes of power storages and their space requirement. Given that the sum of the installed PV and ST areas should not exceed 50% of the building's total roof area ($0.5 \times 396 = 348 \text{ m}^2$), however, a conclusion can be drawn that to keep the E-value unchanged, the solutions associated with the future scenarios (2) and (3) require PV installations to surfaces other than the roof. Alternatively, the analysis suggests, for example, that the E-value of 68.3 kWh/m²,y and the OEF (e) of 0.349 can be obtained in the future scenario (2) with Configuration A by integrating 348 m² of PV panel on the building's roof. This implies that even if the ambitious electrification within the Finnish vehicle stock realizes, harnessing the largest favorable roof area for PV generation would be sufficient for achieving nearly zero-energy goals in the case when transportation energy demand is included in the building's energy balance.

In the present study, ridesharing and modifications in the charging period are proposed as means to affect the energy demand profile of building-related transportation (charging energy) and thus improve the building's energy efficiency and system design. These impacts were examined for the future scenario (2), where the electrification of passenger transportation is ambitious and thus clearly affects the system design. On the other hand, ridesharing and 24-hour charging period is already included in the future scenario (3) as default.

The impact of ridesharing is explained using the proportional increase in the vehicle occupancy in comparison with the reference occupancy (1.9 for highway driving and 1.3 for urban driving), when

the proportions of highway driving (73%) and urban driving (27%) are kept constant. Due to the more efficient use of the vehicle fleet in comparison with the reference case, the occupant-specific energy demand and the hourly average charging power decrease reciprocally (the calculation includes division by the number of passengers), as shown by the graphs at the upper part of Fig. 6. The horizontal axis value 100% refers to a ridesharing mode, where the reference occupancy is doubled (3.8 for highway driving and 2.6 for urban driving).

The visualization at the lower part of Fig. 6 shows the design implications of ridesharing for both the solar PV and the on-site power storage installations as the incremental PV area and power storage in comparison with the reference case (PV area of 200 m², storage capacity 123 kWh). Thus, the data in Fig. 6 suggests, for example, that the PV area required to compensate the EV charging demand reduces from 232 m² (+116%) to 115 m² (+58%), if the vehicle occupancy is doubled. All the values have been calculated for the future scenario (2) and Configuration A with the target E-value of 63 kWh/m²,y and the 7-hour charging period (from midnight to 7:00 AM). The reciprocal change of the occupant-specific energy demand recurs in sizing the PV and power storage. Because the charging period is constant (night-charging), the occupant-specific energy demand (rather than hourly average power) is here the only factor affecting the sizing.

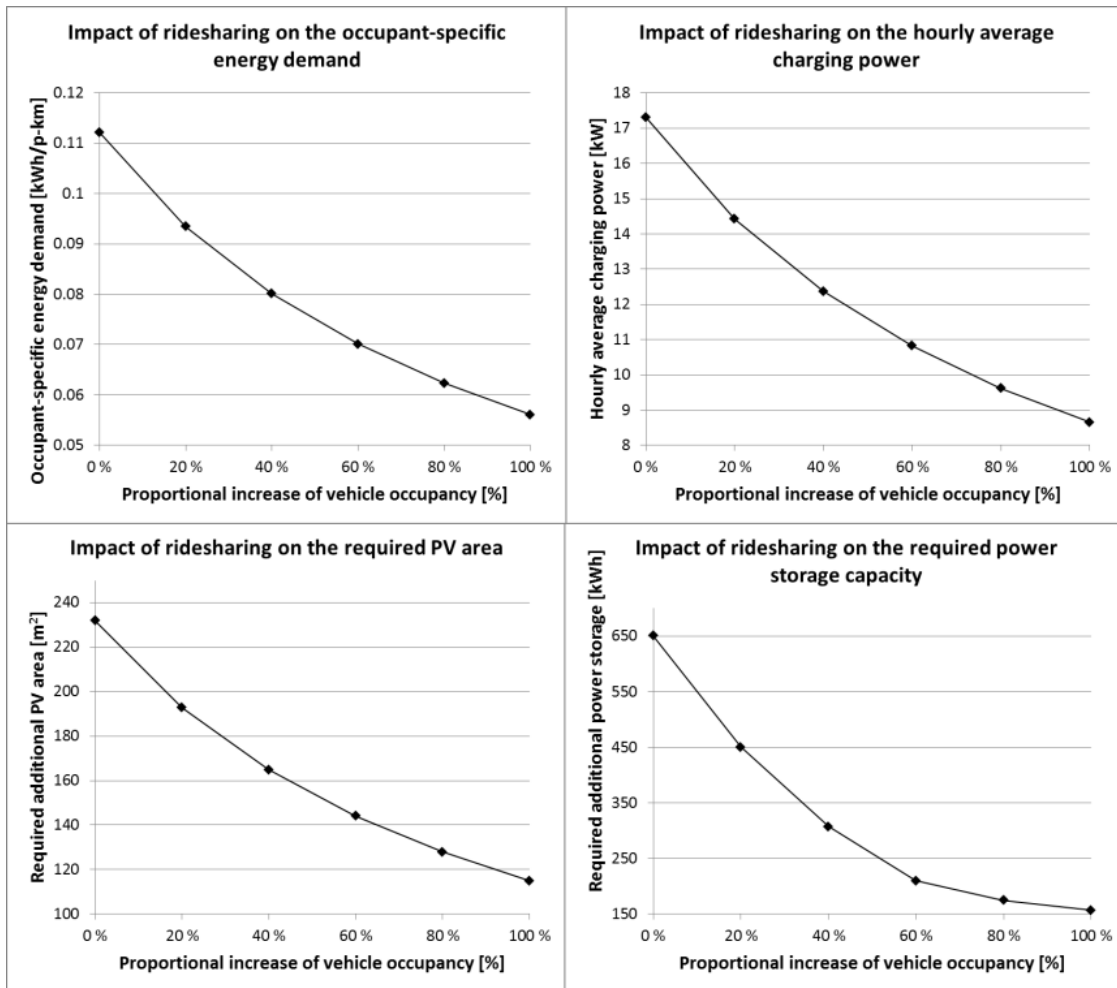


Figure 6. Summary of the design implications of ridesharing.

In contrast to ridesharing, modifying the charging period does not affect the charging energy demand, but it lowers the hourly average charging power demand and smoothens the distribution of charging energy over the hours of a day. On the other hand, the more charging can be repositioned to the hours of daylight, the more efficiently the on-site PV generation can be utilized. The implementation of extended charging periods is justifiable for two main reasons. Firstly, quite an evenly distributed charging throughout the hours of daylight is possible given that the sample population is heterogeneous and the needs of various individuals thus partly cancel out each other (e.g. workers, children, retired individuals). This assumption may be justified by the data in Fig. 7, where the hourly distribution of trips by purpose according to the NTS 2016 has been depicted as percentage. Secondly, extended charging is reasonable as an operational goal, since it enables both

the utilization of affordable off-peak electricity and the maximal direct utilization of on-site power generation.

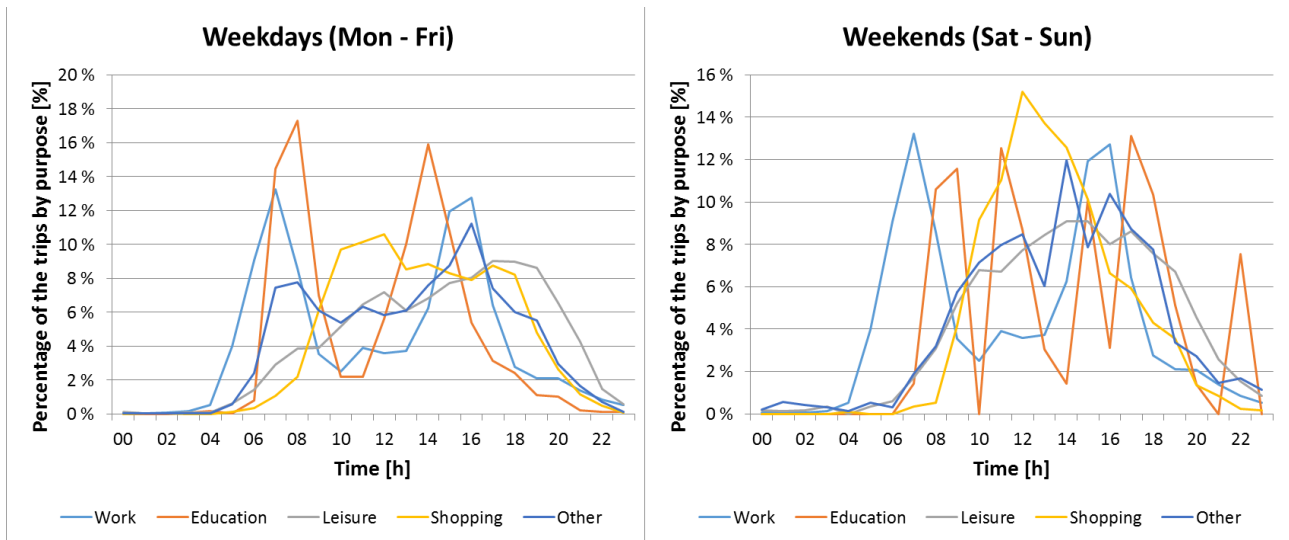


Figure 7. Hourly distribution of trips by purpose [21].

The modification of charging period is examined by way of two different charging schemes, namely, i) the morning scheme (charging starts at midnight) and ii) the evening scheme (charging ends at midnight). These schemes were chosen, since either one of them can be realistically implemented with an assumption that all (or at least the majority) of EV charging takes place via home charging stations, partly during the night hours, when the vehicles are most likely available. Secondly, both of them allow an explicit option to pursue increased utilization of sunlight by adding to the charging time hour by hour. The design implications of extending the charging period from seven (7) hours (reference) to full day (24-hour charging) for both the charging schemes are shown in Fig. 8. All the values have been calculated for the future scenario (2) and Configuration A with the E-value of $63 \text{ kWh/m}^2, \text{y}$.

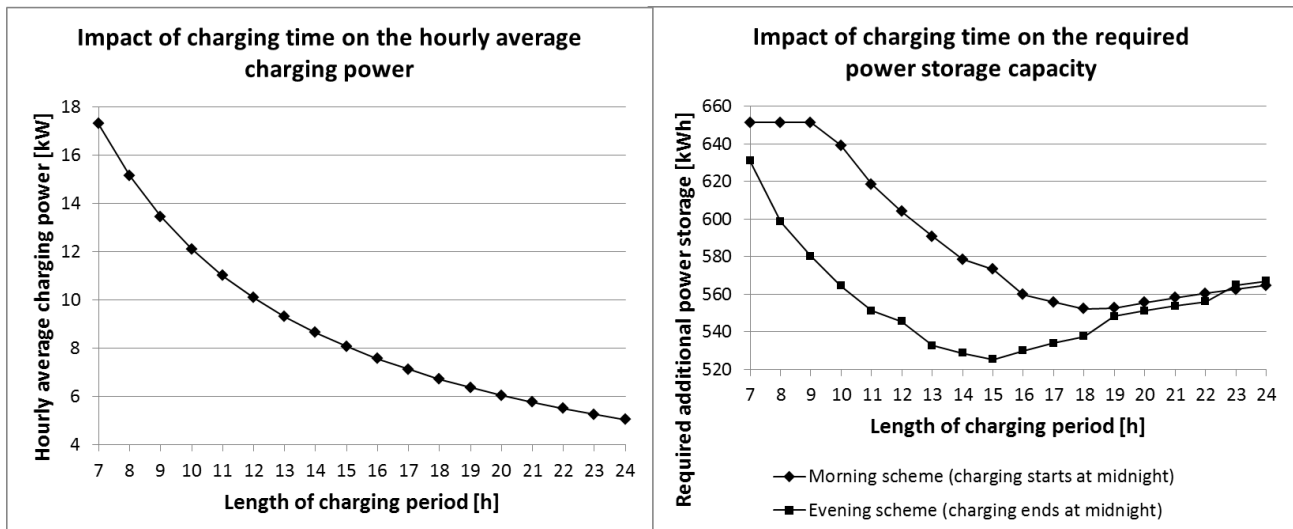


Figure 8. Summary of the design implications of modifying the charging time.

In the left graph in Fig. 8, it is shown that the hourly average charging power decrease reciprocally (the calculation includes division by charging time). The graph on the right side indicates that the more sunlight can be utilized directly by extending the charging hours towards the daylight, the less additional power storage capacity is needed. The most favorable impact is obtained if the charging period can be extended from seven (7) hours to 15-18 hours. This extension is well reasonable, since people commonly work for eight (8) hours and commute just one (1) hour per working day.

Again, it can be concluded that, the evening scheme is preferred in terms of energy performance, since it allows the reduction of up to 120 kWh in comparison with the original 651 kWh of incremental storage capacity in the future scenario (2), Configuration A. The impact of charging schedule on the installed PV area in the aforementioned conditions is quite slight. The PV area can be reduced from the original 432 m² down to 426 m² in the morning scheme and down to 425 m² in the evening scheme in the most favorable conditions.

To find out how the implications of design on seasonal basis differs from those of the design on annual basis, a quarterly analysis was also performed for system configurations A and C and the future scenario (1), which represents a moderate electrification of the vehicle fleet. This analysis indicated clearly the difference between seasonal designs. Regarding the system configuration A,

for example, the incremental PV installation of 298 m² (instead of 67 m² in the sizing on annual basis) is required if the system is designed to maintain in winter conditions (December, January and February) the energy performance equal to that of the building without EV charging requirement. Again, this requirement would result in the power storage capacity demand of >1000 kWh, which would be unreasonably impractical and costly. The conclusion is obvious, since in Finland the solar irradiation remains low during winter months. Correspondingly, the most favorable condition is to size the system on the basis of the power demand during the summer months (June to August). Here, the incremental PV and storage installations are 38 m² and 51 kWh, respectively. The incremental sizing based on fall or spring months is close to the sizing on annual basis. Thus, the study suggests that sizing on the annual basis would enable maintaining the building's energy performance during the majority of the year. Further conclusions would require investigating the design implications on monthly basis, anyway.

As can be inferred from the aforementioned results, the required power storage capacity is one of the critical issues to implement the suggested system. For example, Tesla Powerpack 1 and 2 alone cost some 40,000 € and 70,000 €, respectively (around 400 €/kWh), which makes it preferable to avoid power storage implementation when possible. Given that a bidirectional power interface exists (and power export is thus enabled), the 'no fixed storage' option was also examined. Here, the surplus power is fed into the grid in its entirety and the E-value of the building only increases by 1.8...2.4 kWh/m²,y depending on the system configuration, given that the installed PV area is kept constant (200 m²). The result is a consequence of that there is no credit in Finland for exported non-renewable primary energy, but more energy has to be imported because of impaired match between supply and demand. The absence of the fixed storage reduces the OEF values. For system configuration A, the reduction is 0.043 and for the configuration C it is 0.016. The impact of EV charging energy is minimal in comparison with that of the heating system. In practice, a small fixed

storage would be useful in the case of bidirectional grid-interface, as well, to improve the resilience of the integrated RE systems.

3.4.3 Economic and emission implications

To evaluate the economic implications of including the transportation energy in buildings' energy balance as described in the previous sections, the incremental (difference) capital and life-cycle costs in comparison with the case without transportation energy included in the building's energy balance were calculated for system configurations A and C and the future scenario (1). To estimate the difference life-cycle costs, 25 years was chosen as the system's life span and the discount rate of 3% was used. The acquisition costs for the PV installation was approximated on the basis of the reference [24] as 215 €/panel-m² and the total maintenance costs over the whole analysis period as 6.44 €/panel-m². The electricity price was estimated according to the rate schedule of the local energy utility Helen for households (accessed in January 3, 2019), which provides the day tariff of 7.24 €/kWh and the night tariff of 5.99 €/kWh.

The economic analysis indicated that due to EV charging, the annual electricity costs increase by 774 €/y, which represents 10% increase in the total annual electricity costs with the system configuration A (7,500 €/y without EV charging) and 6% increase with the configuration C (12,400 €/y without EV charging). Correspondingly, the impact of EV charging on the life-cycle costs (25-year period) is 6% in the system configuration A and 5% in the system configuration C, where the power storage costs are lower and the contribution of energy costs is slightly emphasized.

As the E-value equal to that of the case without EV charging included in the energy balance is obtained through incremental PV installation, the annual electricity costs can be reduced by 1% for both system configurations. On the other hand, the incremental PV installation elevates the acquisition and maintenance costs by 33%. Here, the difference life-cycle costs for the system

configurations A and C are 13 €/heated m² (22% increase) and 9 €/heated m² (16% increase), respectively.

Presumptively, the modification of the charging period provides some benefit in terms of electricity costs so that the morning scheme is more viable since charging is mostly scheduled into the night hours. Here, the difference between the morning scheme and the evening scheme with 7 h charging period is 68 €/y. The difference between these two schemes fades out in tandem with increasing length of the charging period. Thus, one can conclude that the impact of the charging strategy is less than 9% in comparison with the incremental electricity costs due to EV charging (774 €/y).

The implications on the CO₂ emissions were estimated using the specific emission factors for grid electricity (0.164 kg_{CO2}/kWh) and district heat (0.182 kg_{CO2}/kWh). These specific emissions are acquired from the data of Statistics Finland from 2016. Without the EV charging, the CO₂ emissions for the system configurations A and C are 14.6 and 8.5 kg/heated m², y, respectively. The difference is explained by the presence of district heating in the configuration C. Correspondingly, the impact of EV charging on the CO₂ emission is 4% in the system configuration A and 7% in the system configuration C.

3.4.4 Discussion

The methodology presented in Section 2 and demonstrated by the case study in Section 3 takes a new perspective into combining statistical data collected on regular basis and the estimation of building energy demand using whole-building simulation. Particularly, the approach is proposed to be routinely used in early-stage design. The proposed method is transparent in itself, wherefore it is also compatible with building sustainability certifications, such as LEED.

The data obtained from the case study suggest that transportation energy, identified as the EV charging requirement, is likely to be relevant from the viewpoint of buildings' energy performance. It will remarkably affect the sizing of renewable energy systems and thus should be accounted as

building-related energy demand in a buildings' energy balance. The results can be generalized to similar type of buildings and communities located in demographically and climatically similar areas. For the sake of prevalence, the energy demands and E-values are commonly expressed per heated square meter or occupancy of a building. In analyses akin to one described in previous sections, this approach is suggested to be extended to all transportation-specific energy demands, which contribute to the building's energy performance or system sizing.

For the implementation of a statistical approach, the size and the characteristics of the target community's population is relevant, since it signifies a representative sample among all the individuals living in similar conditions. Therefore, the usability of the suggested approach can be improved if the population of the building is large and diverse enough, as may be the case with large apartment buildings. Inversely, if the design problem concerns a single-family house, a more preferable approach would be to pursue information about the predicted occupant behavior, for example, through activity-based modeling. Regarding the data on occupant-specific daily travel distances obtained from the NTS 2016, the sample size of around 7,000 has been applied to the analysis covering the inhabitants living in the Helsinki Metropolitan area [21]. Here, the estimated variation of daily travel distances by passenger cars is $\pm 6.5\%$ around the reference value 21.8 p-km/day (95% confidence level). Again, on the basis of the theory of statistics, the margin of error taking into account the sample size of 124 occupants is $\pm 8.8\%$ (95% confidence level).

The data on specific energy demands of passenger cars in the LIPASTO database is based on the documentation on the vehicle-specific energy consumption provided by the Finnish Transport and Communications Agency (Trafi). Uncertainty is caused by biases between reported and actual energy demands. Especially during winter, vehicle heating may significantly increase the energy consumption of electric cars. Determining the specific energy demand incorporates the entire national vehicle stock, wherefore statistical error comparable to that related to occupant-specific travel distance exists. Concerning the essence of the present study as a scenario analysis, however,

it is recognized that the future scenarios are tentative and predictive. Therefore, an attempt to take into account the uncertainty has been made by analyzing a variety of possible developments. Due to the rapid and hardly predictable evolution of the technology and economy related to prime movers, the development of vehicle-specific travel distances should be done on conservative basis.

Regarding the calculation of building's net energy demand, the dynamic IDA-ICE simulation software has performed well in several validation studies [e.g. 31, 32]. Here, the performance of the tool in itself has been tested against measured data following standardized procedures. The most likely sources of error are due to external reasons such as improper input data and post-processing the results. The method would particularly benefit from hourly data on the usage of electric appliances and lighting, which should be used instead of specific demands.

The future prospects for the suggested approach are favorable, since due to the Internet-of-Things (IoT), the data collection from both the vehicle stock and the building stock can be automated and the possibilities to combine various databases improve. Here, for example, extensive mobility data can be collected through mobile devices instead of laborious interviews. Correspondingly, data on hourly demands can be routinely collected through building automation systems and combined into databases for given building types. Yet, several issues such as data security and ownership are partly unresolved.

4 Conclusions

The research reported in this article hypothesized that the electrification of passenger cars has a remarkable impact on dimensioning building-integrated renewable energy systems and it should be addressed when pursuing zero-energy goals. Since a lack of useful approaches to quantify the impacts of vehicle-specific energy demands and occupant-specific mobility requirements in single buildings' energy balance was observed, a statistically-inspired, occupant-specific model was developed to facilitate the early-stage design of large residential buildings' energy systems. The

suggested model is useful particularly because it is simple and transparent, it utilizes standardized calculation methods and energy demand data collected routinely and regular basis.

The model was implemented in a case study involving a new Finnish apartment building and three possible future scenarios depicting moderate, ambitious and hypothetical electrification of the Finnish passenger vehicle stock. The results of the case study suggest that in the future, the transportation energy demand should be taken into account in the design of large residential buildings' energy systems even if the electrification of the Finnish vehicle stock is moderate (250,000 EVs in the stock of approximately 3,000,000 passenger cars by 2030). Here, the transportation energy accounts for 6-10% of the delivered energy and 6-7% of the E-value, but maintaining the building's energy performance comparable to the case with no vehicle charging included, the solar PV system should be sized up to 34% and the building-integrated electrical storage capacity up to 72% larger. In the ambitious scenario (800,000 EVs), the corresponding percentages are 19-28% for the delivered energy and 19-20% for the E-value, whereas the solar PV area should be increased by more than 100%.

The results of the case study are always case-specific, but yet they suggest that similar conclusions could be drawn by analyzing similar buildings located in similar climatic and demographic areas. One should note that particularly in the specific case where the E-value obtained through cost optimization is close to a pre-defined reference value for nearly zero-energy buildings, the impact of transportation energy demand should be investigated. The representativeness of the analysis presented in this article should be tested in the future research by investigating various buildings in various demographic and climatic regions as well as more detailed profiles regarding the occupant behavior (e.g. activity- or agent-based modeling). Integrating the data collected via smart vehicles and building automation systems with an aim to create user mobility profiles also provides an attractive topic for the future research. Given that the future buildings and communities may also shape energy cooperatives, the design implications of smart load management and the utilization of

the EV's battery storages as well as building-specific vehicle fleet composition, scheduling and routing problems would also provide interesting research opportunities.

References

- [1] Energy Efficiency Trends in the EU / Key messages. Lessons from the Odyssee-Mure Project. 2013.
- [2] EPBD recast, Directive 2010/31/EU of the European Parliament and of the Council of 19 May 2010 on the energy performance of buildings (recast), Official Journal of the European Union, (2010) 18/06/2010.
- [3] Amaral, A.R., Rodrigues, E., Gaspar, A.R., Gomes, Á., Review on performance aspects of nearly zero-energy districts, Sustainable Cities and Society 2018, Vol. 43, pp. 406-420.
- [4] Saheb, Y., Shnapp, S. Johnson, C., The Zero Energy concept: making the whole greater than the sum of the parts to meet the Paris Climate Agreement's objectives, Current Opinion in Environmental Sustainability 2018, Vol. 30, pp. 138-150.
- [5] Marique, A.-F., Reiter, S.A., Simplified framework to assess the feasibility of zero-energy at the neighborhood/community scale, Energy and Buildings 2014, Vol. 82, pp. 114-122.
- [6] Amirioun, M.H., Kazemi A., A new model based on optimal scheduling of combined energy exchange modes for aggregation of electric vehicles in a residential complex, Energy 2015, Vol. 69, pp. 186-198.
- [7] Grazia Speranza, M., Trends in transportation and logistics, European Journal of Operational Research 2018, Vol. 264, pp. 830-836.
- [8] Renault Symbioz. (URL: <https://www.renault.co.uk/vehicles/concept-cars/symbioz-concept.html>)

- [9] Doroudchi, E., Alanne, K., Okur, Ö., Kyyrä, J., Lehtonen, M., Approaching net zero energy housing through integrated EV, *Sustainable Cities and Society* 2018, Vol. 38, pp. 534-542.
- [10] Osório, B., McCullen, N., Walker, I., Cole, D., Integrating the energy costs of urban transport and buildings, *Sustainable Cities and Society* 2017, Vol. 32, pp. 669-681.
- [11] Stephan, A., Stephan, L., Life cycle energy and cost analysis of embodied, operational and user-transport energy reduction measures for residential buildings, *Applied Energy* 2016, Vol. 161, pp. 445-464.
- [12] Marique, A.-F., de Meester, T., De Herde, A., Reiter, S., An online interactive tool to assess energy consumption in residential buildings and for daily mobility, *Energy and Buildings* 2014, Vol. 78, pp. 50-58.
- [13] Nsaliwa, D., Vale, R., Isaacs, N., Housing and Transportation: Towards a Multi-scale Net Zero Emission Housing Approach for Residential Buildings in New Zealand, *Energy Procedia* 2015, Vol. 75, pp. 2826-2832.
- [14] Karan, E., Mohammadpour, A., Asad, S., Integrating building and transportation energy use to design a comprehensive greenhouse gas mitigation strategy, *Applied Energy* 2016, Vol. 165, pp. 234-243.
- [15] Marique, A.-F., Reiter, S.A., A method for evaluating transport energy consumption in suburban areas, *Environ. Impact Assess. Rev.* 2012, Vol. 33, pp. 1-6.
- [16] Wang, A., Stogios, C., Gai, Y., Vaughan, J., Ozonder, G., Lee, S.J., Posen, I.D., Miller, E.J., Hatzopoulou, M., Automated, electric, or both? Investigating the effects of transportation and technology scenarios on metropolitan greenhouse gas emissions, *Sustainable Cities and Society* 2018, Vol. 40, pp. 524-533.

- [17] EU 244/2012 Commission Delegated Regulation No244/2012 of 16. Supplementing Directive 2010/31/EU of the European Parliament and of the Council on the energy performance of buildings by establishing a comparative methodology framework for calculating cost-optimal levels of minimum energy performance requirements for buildings and building elements (January 2012).
- [18] Kurnitski, J., Saari, A., Kalamees, T., Vuolle, M., Niemelä, J., Tark, T., Cost optimal and nearly zero (nZEB) energy performance calculations for residential buildings with REHVA definition for nZEB national implementation, *Energy and Buildings* 2011, Vol. 43, pp. 3279-3288.
- [19] Cao, S., Hasan, A., Sirén, K., On-site energy matching indices for buildings with energy conversion, storage and hybrid grid connections, *Energy and Buildings* 2013, Vol. 64, pp. 423-438.
- [20] LIPASTO 2017, Calculation system for traffic exhaust emissions and energy use in Finland. (URL: <http://lipasto.vtt.fi/en/index.htm>).
- [21] Finnish Transport Agency. National Travel Survey 2016.
- [22] D3 Finnish code of building regulation, Rakennusten energiatehokkuus (Energy efficiency of buildings), Regulations and guidelines 2012, Helsinki, Finland, 2011. [In Finnish].
- [23] D5 Finnish code of building regulation, Rakennusten energiankulutuksen ja lämmitystehontarpeen laskenta (Calculation of power and energy needs for heating of buildings), Guidelines 2012, Ministry of the Environment, Helsinki, Finland, 2013. [In Finnish]
- [24] Häkämies, S. (Ed.), Heat pumps in energy and cost efficient nearly zero energy buildings in Finland, VTT Technology 235. VTT Technical Research Centre of Finland Ltd. Espoo, Finland, 2015, 109 p. ISBN 978-951-38-8356-0 (URL: <http://www.vttresearch.com/impact/publications>).

- [25] Tuominen, A., Tervonen, J., Järvi, T., Mäkelä, K., Liimatainen, H., Nykänen, L., Rehunen, A., Liikenteen energiatehokkuustoimenpiteet osana EU:n 2030 ilmasto- ja energiatavoitteiden saavuttamista: vaikutukset, kustannukset ja työnjako, Valtioneuvoston selvitys- ja tutkimustoiminnan julkaisusarja 14, Helsinki, Finland, 2015, 61 p. ISBN PDF 978-952-287-193-0. [In Finnish].
- [26] Lahtinen, S., Tuominen, J., Kokkonen, M., Liikennesuoritelaskenta vuodelle 2017 (Traffic performance calculations for 2017), Statistics Finland, Helsinki, Finland 2018. 28 p. [In Finnish]
- [27] Granskog, A., Gulli, C., Melgin, T., Naucler, T., Speelman, E., Toivola, L., Walter, D., Cost-efficient emission reduction pathway to 2030 for Finland. Opportunities in electrification and beyond, Sitra studies 140. Sitra, Helsinki, Finland 2018. 78 p. ISBN 978-952-347-082-8.
- [28] Linturi, R., Loppuraportti: Automaattisen liikenteen metropolivisio (Final report: Metropolitan Vision of Automatic Transportation), FC Sovelto Oyj, Helsinki, Finland 2013. 40 p. [In Finnish]
- [29] Reinikainen, E., Loisa, L., Tyni, A., FInZEB hanke – Lähes nollaenergiarakennusten käsitteet, tavoitteet ja suuntaviivat kansallisella tasolla (Defining 'nearly zero' in Finland – FInZEB), FInZEB – Final report 2015, 71 p. [in Finnish]
- [30] Bishop, J.D.K., Doucette, R.T., Robinson, D., Mills, B., McCulloch, M.D., Investigating the technical, economic and environmental performance of electric vehicles in the real-world: A case study using electric scooters, Journal of Power Sources 2011, Vol. 196, pp. 10094-10104.
- [31] Achermann, M., Zweifel, G., RADTEST – Radiant heating and cooling test cases, Subtask C. A Report of IEA Task 22: Building Energy Analysis Tools, 2003.
- [32] Kropf, S., Zweifel, G., Validation of the building simulation program IDA-ICE according to CEN 13791 'Thermal performance of buildings—calculation of internal temperatures of a room in summer without mechanical cooling—general criteria and validation procedures', Luzern, 2001.